Optik - International Journal for Light and Electron Optics 176 (2019) 132–142

Contents lists available at ScienceDirect

Optik

journal homepage: www.elsevier.com/locate/ijleo

Original research article

Development of CZTGS/CZTS tandem thin film solar cell using SCAPS-1D

Adeyinka D. Adewoyin*, Muteeu A. Olopade, Olusola O. Oyebola, Micheal A. Chendo

Department of Physics, University of Lagos, Akoka, Lagos, Nigeria

ARTICLE INFO

Keywords:
Efficiency
CZTGS/CZTS
Optimization
Tandem
Thin film

ABSTRACT

In this work, numerical modeling and simulation of a monolithic CZTGS/CZTS tandem structure has been carried out using SCAPS-1D. This is aimed at enhancing the performance of copper zinc tin sulfide (CZTS) solar cell using a double junction CZTGS/CZTS tandem structure. The top cell consists of a non-toxic element (germanium) used in tuning the band gap of copper zinc tin germanium sulfide (CZTGS) while the bottom cell is CZTS based. The best J–V characteristics of the top cell was obtained at a composition ratio of $Cu_2ZnSn_{0.8}Ge_{0.2}S_4$ with an efficiency of 9.39%. The bottom cell condition is simulated based on the state-of-art records with an efficiency of 8.4% which is in good agreement with experimental results. At an absorber thickness of 0.65 μm and 3.00 μm of the top and bottom sub-cell of the tandem structure under current matching condition of 18.53 mA/cm^2 gave an efficiency of 17.51%. This is a significant improvement in efficiency over that of the CZTS thin film solar cell with a single junction.

1. Introduction

In response to the development of a tandem solar cell that could satisfy the standard requirement of photovoltaic cells (PVs) such as low cost of materials and fabrication, non-toxic and readily available constituent elements and high conversion efficiency without material degradation [1,2], a suitable absorber layer material for thin film solar cells has to be developed. Currently, thin film technology is receiving more attention than the traditional wafer technology because of its much lower material usage and cost of production which is the goal of PV technology [3,4].

In today's PV market, there are thin film solar cells (TFSC) such as copper indium gallium disulfide (CIGS) and cadmium telluride (CdTe) that are already competing with the silicon solar cells. However, these TFSCs has some major drawbacks. The skyrocketing material cost and scarcity of indium and gallium is a major setback for the CIGS thin film solar cell despite the fact that it has attained an efficiency of 22.6% with high stability. Also, the toxicity of selenium in CIGSSe and cadmium in CdTe is another problem to their development even though CdTe TFSC is equally stable with an efficiency of 22.1% [5,6]. It has been predicted that these major setbacks for CIGS and CdTe will limit its mass production, deployment and economic sustainability [1].

To this end, an alternative absorber layer material for TFSC has to be sought for in order to overcome these major challenges in the existing ones. One promising absorber material is the $Cu_2Zn(Sn,Ge)(S,Se)_4$ (CZTGSSe) due to its high absorption coefficient, direct and optimal band gap coupled with the fact that its physical properties can be tailored by changing the composition of Sn and Ge as well as S and Se [5,7]. Efficiency as high as 12.6% has been achieved for CZTSSe based solar cells [8]. Since, our focus is to develop a selenium (toxic) free solar cell, a pure CZTGS/CZTS based TFSC will be the most appropriate. However, the record efficiency of about

* Corresponding author.
E-mail address: dadeyinka@unilag.edu.ng (A.D. Adewoyin).

https://doi.org/10.1016/j.ijleo.2018.09.033
Received 16 March 2018; Received in revised form 8 September 2018; Accepted 9 September 2018

10% obtained for a single junction CZTS solar cell is still very low when compared to its theoretical efficiency of 28% [6,9]. The excellent properties of Cu_2ZnSnS_4 (CZTS) quaternary compound makes it as promising material as the absorber layer for thin film solar cells (TFSCs). CZTS has a high absorption coefficient of over $10^4\,cm^{-1}$ and a direct and optimal band gap of about 1.5 eV [8–10].

Consequently, this research work will focus on the enhancement of the conversion efficiency of a single junction CZTS solar cell. To achieve this, a monolithic (double junction) tandem structure is considered since multi junction solar cells are useful for better photon absorption and improved efficiency with the modification of the structure of the cells and semiconductor material properties [11]. The monolithic tandem structure consists of CZTGS top cell absorber layer material and CZTS bottom cell absorber layer material. To this end, a systematic enhancement of the device through the tuning of the band gap and the variation of the electron affinity is carried out in order to determine the optimal band gap with its corresponding electron affinity of the CZTGS top cell. The control of the bandgap of CZTGS was made possible through the variation of Ge/(Sn + Ge) ratio to form $Cu_2ZnSn_{1-x}Ge_xS_4$. The introduction of Ge is of better advantage in the tuning of the bandgap of CZTS because it is non-toxic like Se in the case of CZTSSe. The numerical simulation of CZTS bottom cell is carried out and compared with the previously reported experimental result. Finally, the effect of temperature variation on the tandem solar cell was simulated and analyzed.

2. Methodology

In this work, we made use of the Solar Cell Capacitance Simulator (SCAPS-1D) software, version 3.3.05 [12], which is one of the most renowned applications in the modeling and simulation of thin film polycrystalline solar cells. It is a one-dimensional program developed at the Department of Electronics and Information Systems, Gents University, Belgium and has been designed to simulate the electrical characteristics under the dark and light illumination at different operating temperatures. At present, this software has been tested for the stable thin film solar cells such as CdTe and CIGS [13–15]. Also, SCAPS software has been reported in literatures for the modeling and simulation CZTS thin film solar cells [7,16]. Hence, numerical simulation will be an essential tool in studying the input to experimental optimization and further evaluation of the performance characteristics of CZTS solar cells.

Basically, a numerical program that can be used as modeling tool aimed at the simulation of the properties of semiconductor structures must be able to solve the basic semiconductor equations. These semiconductor equations include the Poisson equation which relates the electrostatic potential to charge (Eq. (1)), continuity equation for electrons (Eq. (2)) and continuity equation for holes (Eq. (3)).

$$\frac{\partial}{\partial x}\left(\varepsilon_o\varepsilon_r\frac{\partial \Psi}{\partial x}\right) = -q\left(p - n + N_D^+ - N_A^- + \frac{\rho}{q}\right) \tag{1}$$

$$-\left(\frac{1}{q}\right)\frac{\partial J_n}{\partial x} - U_n + G = \frac{\partial n}{\partial t} \tag{2}$$

$$-\left(\frac{1}{q}\right)\frac{\partial J_p}{\partial x} - U_p + G = \frac{\partial p}{\partial t} \tag{3}$$

Where Ψ is the electrostatic potential, ε_o is the permittivity of free space and ε_r relative permittivity, ρ is the charge density of defects, n and p are the free carrier concentrations while N_D^+ *and* N_A^- are the densities of the ionized donors and acceptors, G is the generation rate, J_n and J_p are the electron and hole current densities.

Using appropriate boundary conditions at the interfaces and contacts, these set of equations results in a system of coupled differential equations which when solved, solar cell device parameters like the open-circuit voltage (V_{oc}), short circuit current density (J_{sc}), fill-factor (FF), and the efficiency (η) can be determined. The modeled structure of the top cell consists of ZnO:Al, CdS, CZTGS, Molybdenum thin film layers which are the window, buffer, absorber, back contact layers respectively as shown in Fig. 1. Similarly, the bottom cell consists of ZnO:Al, CdS, CZTS, Molybdenum thin film layers which are the window, buffer, absorber, back contact layers respectively as shown in Fig. 2. The top and bottom cell structure is assumed to be deposited on a soda lime glass (SLG) substrate [17]. These model structures were implemented on the SCAPS simulation software using the material and device parameters (baseline) of Tables 1 and 2 respectively. These parameters in the simulation were obtained from theories, literature values and in some cases reasonable estimates were made were exact experimental values are not available [18–22].

The absorption files used in the simulation define the absorption coefficient due to different wavelengths and the variation of $(h\nu\alpha)^2$ as a function of photon energy, $(h\nu)$ for CZTS thin film is shown in the work of Patel and Ray [18]. The minority carrier lifetime (τ) of CZTS solar cells from time resolved photoluminescence is approximately 8 ns while the estimated lower bound of the diffusion length (Ln) of the electrons is given as 350 nm [23].

A higher efficiency than those for a single junction solar cell can be obtained by stacking together different absorbers with different band gaps to maximize the light absorption. The concept of monolithic tandem cell is based on a stack of solar cells with the same optical target. The cells are connected in series according to semiconductor energy gap, where each cell absorbs the range of the solar spectrum that corresponds to its gap [24]. In this work, the basic structure of CZTGS/CZTS tandem solar cell is shown in Fig. 3. The top and bottom sub cells are optically and electrically connected through a tunnel junction. The tunnel junction is a n/p junction which actually functions as a recombination junction. For a highly stabilized efficiency in tandem cell applications, a good n/p junction must have very high recombination rates, negligible optical absorption, and an ohmic characteristic with a low series

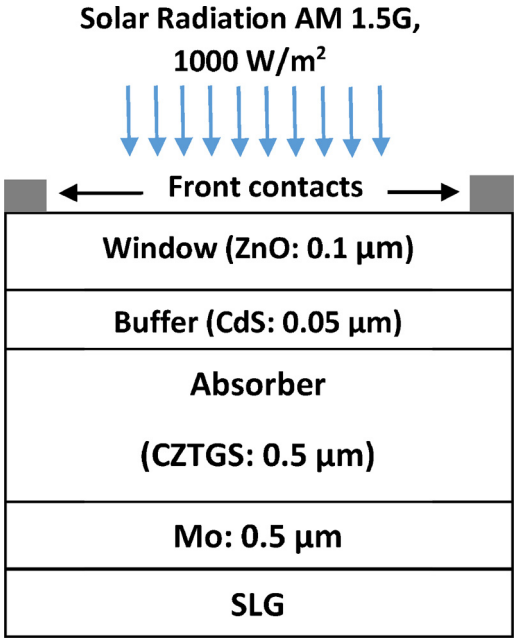

Fig. 1. Schematic of single CZTGS top cell.

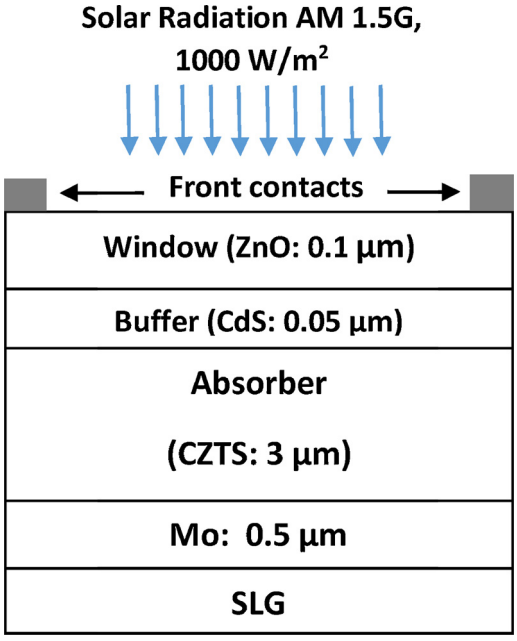

Fig. 2. Schematic of single CZTS bottom cell.

resistance in order to improve the carrier transport [25]. However, due to the series connection of a monolithic tandem cell, its efficiency is limited by the solar cell that issues the lower current. Consequently, a current matching condition among the cells building the tandem, must be achieved. This can be achieved by adjusting the top cell absorber thickness to an optimal value where the short circuit current densities of the top, bottom and tandem cells are similar [26,27].

Under illumination, free carriers are generated and the Fermi level split into quasi Fermi level since this is a thin film device with a heterojunction [18]. The separation between quasi-Fermi level is responsible for V_{oc} of the device while short circuit current (J_{sc}) is a function of the solar spectral irradiance. The flat band was used for the front contact. SCAPS application package automatically calculates the values of the work function when a flat band is used for the simulation [13]. A work function of 5 eV was considered for Molybdenum (Mo) which serves as the back contact. Mo was considered because of its excellent conductivity and high optical reflectivity to reflect photons back into the absorber layer [28]. The data obtained from the various simulations of the devices using

Table 1
Basic material parameters used in the simulation.

Material Properties	Window Layer (AZO)	Buffer Layer (CdS)	Absorber layers		Tunnel Junction	
			CZTS	CZTGS	p+ −CZTGS	n+ −CZTS
Thickness (μm)	0.1	0.05	3.0	0.5	0.025	0.025
Bandgap (eV)	3.3	2.4	1.5	1.59	1.59	1.5
Electron Affinity (eV)	4.6	4.2	4.5	4.19	4.19	4.5
Dielectric permittivity ε	9	10	10	10	10	10
Conduction band effective density of states (cm^{-3})	2.2×10^{18}	1.8×10^{19}	2.2×10^{18}	2.2×10^{18}	2.2×10^{18}	2.2×10^{18}
Valence band effective density of states (cm^{-3})	1.8×10^{19}	2.4×10^{18}	1.8×10^{19}	1.8×10^{19}	1.8×10^{19}	1.8×10^{19}
Electron mobility (cm^2/Vs)	100	100	60	60	60	60
Hole mobility(cm^2/Vs)	25	25	20	20	20	20
Donor density N_D (cm^{-3})	1×10^{18}	1×10^{17}	10	10	10	1×10^{19}
Acceptor density N_A (cm^{-3})	1×10^{5}	10	7×10^{16}	7×10^{16}	1×10^{20}	10
Defect type at bulk/interface			Donor/Neutral	Donor/Neutral		
Absorption coefficient ($cm^{-1}\,eV^{1/2}$)	SCAPS data	SCAPS data	4.25×10^{4}	4.25×10^{4}	4.25×10^{4}	4.25×10^{4}

Table 2
Basic device parameters used in the simulation.

Cell Properties		
Cell temperature		300 K
Series resistance R_s		4.25 Ωcm^2
Shunt resistance R_{sh}		$4 \times 10^2\,\Omega cm^2$
Contacts	**Front metal contact**	**Back metal contact**
Work function	Flat band	Mo 5 eV
SRV of electron	10^7 cm/s	10^7 cm/s
SRV of hole	10^7 cm/s	10^7 cm/s

SRV: Surface Recombination Velocity.

the SCAPS-1D were exported to Microsoft Excel 2016 to plot the graphs.

3. Results and discussion

The results presented in this section are arranged in a systematic order beginning with the independent modeling and simulation of the top and bottom device of the tandem solar cell. Secondly, a combination of the top and bottom layer into a monolithic tandem structure was modeled and simulated. Lastly, the result of the effect of temperature variation on the tandem device is presented.

3.1. Modeling and simulation of a single CZTS thin film solar cell

The modeling and simulation of the bottom cell with the schematic shown in Fig. 2 was conducted using the baseline parameters (Tables 1 and 2). In this case, CZTS served as our absorber layer material. The current voltage characteristics is shown in Fig. 4. The simulation of the device gave an efficiency (η) of 8.42%, an open circuit voltage (V) of 0.68 V, short circuit current (J) of 19.72 mA/cm^2 and the fill factor (FF) of 62.72%. This result is in good agreement with the experimental result reported by Shin et al. [23]. The J–V characteristic of their best performing CZTS-based solar cell had an efficiency of 8.4% with open circuit voltage of 0.66 V, short circuit current density of 19.50 mA/cm^2, fill factor of 65.80%. Thus, validating the model and the parameters chosen for the simulation.

3.2. Modeling and simulation of a single CZTGS thin film solar cell

To model and simulate CZTGS thin film solar cell for the bottom layer device, the band gap of the bulk material was first tuned and their corresponding electron affinities were determined. The tuning is imperative because the composition ratio of Sn and Ge that will give the best performance which makes it suitable as the top sub-cell needs to be determined. The results obtained were subsequently optimized to determine the best performing device for the CZTGS thin film solar cell. The steps taken to achieve these results are as follows:

3.2.1. Tuning of the band gap

As mentioned previously, the band gap of CZTGS layer along with its corresponding electron affinity can be varied according to the change in 'x' content of the structure, $Cu_2ZnSn_{1-x}Ge_xS_4$. Through this, the optimal value of the band gap and electron affinity of

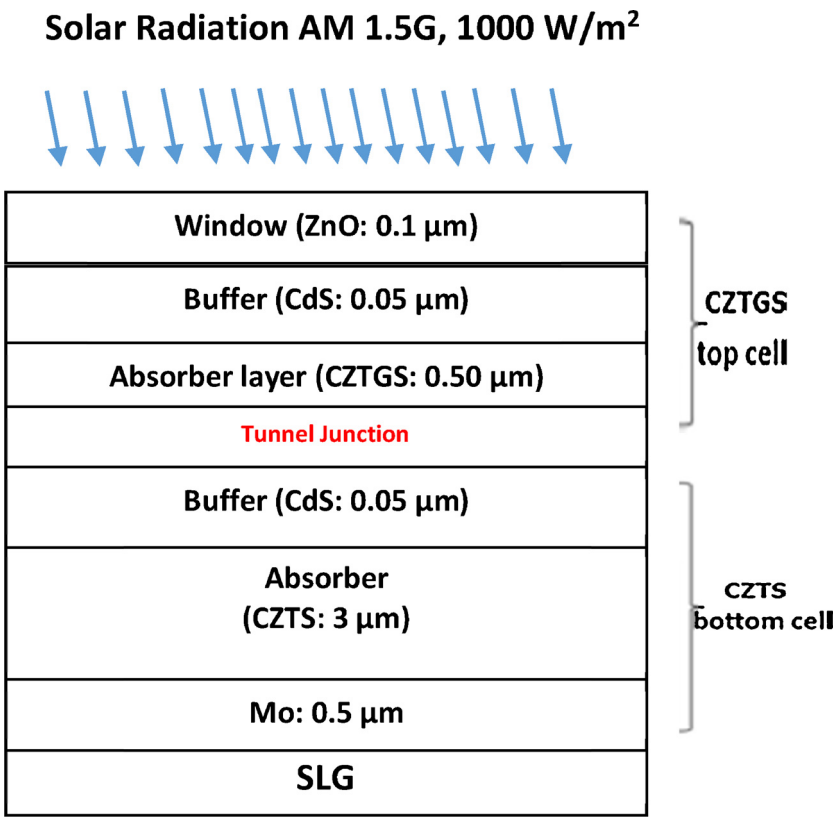

Fig. 3. Schematic of CZTGS/CZTS tandem solar cell.

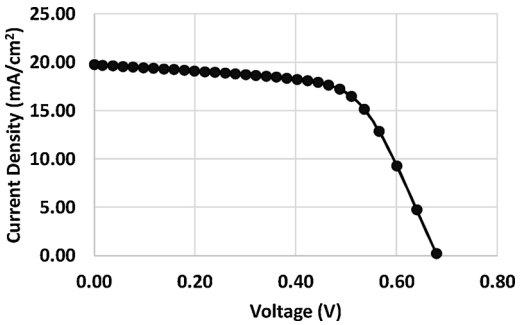

Fig. 4. J–V plot of base model of CZTS solar cell.

CZTGS can been determined. The band gaps of CZTGS used in this study were obtained from the experimental work of Singh et al. and Khadka & Kim [29,30] and the average of their results was determined and was further used to compute their corresponding electron affinities with respect to the variation of "x" in the composition of the compound as shown in Table 3a. The electron affinities were determined from Eq. (4) based on the values of the barrier height obtained from the simulation of the model based on their corresponding values of band gap. Details of this equation has been reported in the work of Adewoyin et al. and Kodigala [31,32]

Table 3a
Band gap and electron affinity of $Cu_2ZnSn_{1-x}Ge_xS_4$ alloy composition.

Ge/(Sn + Ge) ratio, x	Band gap (eV) Singh et al., 2016	Band gap (eV) Khadka & Kim, 2015	Average Band gap (eV)	Electron Affinity (eV)
0	1.54	1.51	1.53	4.35
0.30	1.65	1.59	1.62	4.12
0.50	1.74	1.67	1.71	3.97
0.70	1.85	1.79	1.82	3.82
1.00	1.98	1.91	1.95	3.67

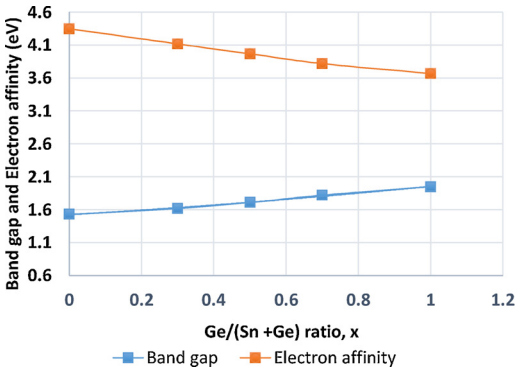

Fig. 5. Variation in band gap and electron affinity due to change in Ge content of CZTGS composition.

$$\phi_b = E_g - (\phi_m - \chi) \tag{4}$$

Where ϕ_b is the barrier height, E_g is the band gap of the semiconductor, ϕ_m is the metal work function of the semiconductor and χ is the electron affinity of the semiconductor (CZTGS).

Generally, it was observed that as the band gap increases, the electron affinity decreases with the rising of 'x' values.

Using appropriate curve fitting of Fig. 5, the mathematical Eqs. of (5) and (6) can be derived from Table 3a.

$$E_g = 1.5248 + 0.324x + 0.107x^2 \tag{5}$$

$$\chi = 4.3544 - 0.8656x + 0.176x^2 \tag{6}$$

3.2.2. Effect of absorber layer band gap variation on cell efficiency

Keeping the other solar cell parameters constant, the band gap of $Cu_2ZnSn_{1-x}Ge_xS_4$ is varied from 1.53 eV to 1.95 eV. Using Eqs. 5 and 6, the band gaps and electron affinities of CZTGS whose variation of x composition is not in Table 3a is calculated. Then the current density, voltage, fill factor and efficiency of the corresponding variation in x is determined through the simulation of the device as shown in Table 3b.

From Table 3b, it is generally observed that the best performance of the device was obtained at a composition ratio of $Cu_2ZnSn_{0.8}Ge_{0.2}S_4$. As the band gap begins to increase beyond the composition ratio of x = 0.2, the fill factor begins to reduce significantly and this degrades the quality of the solar cell significantly. The higher the bandgap, the lower will be the saturation current density and since the saturation current density is a measure of the recombination of minority carriers across the p-n junction, the series resistance will increase [33]. Consequently, the short circuit current decreases. The corresponding J–V characteristics of this best performing device is shown in Fig. 6.

The solar cell parameters deduced from the calculated J–V curve of Fig. 6 are;

$V_{oc} = 0.86$ V

$J_{sc} = 17.39$ mA/cm^2

FF = 63.61%

$\eta = 9.39\%$

3.3. Modeling and simulation of a single layer CZTGS/CZTS thin film solar cell

The schematic of CZTGS/CZTS solar cell tandem structure is shown in Fig. 3. This design is a double junction, monolithic tandem

Table 3b
Band gap and electron affinity of $Cu_2ZnSn_{1-x}Ge_xS_4$ alloy composition.

Ge/(Sn + Ge) ratio, x	Average Band gap (eV)	Electron Affinity (eV)	V_{oc} (V)	J_{sc} (mA/cm^2)	FF (%)	η (%)
0	1.53	4.35	0.68	19.72	62.72	8.42
0.1	1.56	4.27	0.76	18.17	64.26	8.89
0.2	1.59	4.19	0.86	17.39	63.61	9.39
0.3	1.62	4.12	1.30	16.76	43.95	9.61
0.4	1.67	4.04	1.93	15.64	30.48	9.20
0.5	1.71	3.97	1.98	14.80	29.64	8.69
0.6	1.76	3.90	1.96	13.69	29.76	7.99
0.7	1.82	3.82	1.93	12.58	30.00	7.28
0.8	1.85	3.77	1.90	11.77	30.17	6.77
0.9	1.90	3.72	1.87	11.10	30.37	6.32
1.0	1.95	3.67	1.41	10.24	40.29	5.80

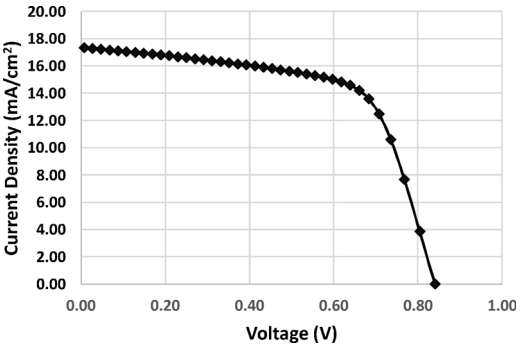

Fig. 6. J–V plot of base model of CZTS solar cell.

structure. The cells are connected in series and arranged according to their energy band gaps. The band gaps of the tandem cells are selected in such a way that it could absorb the maximum effective solar flux. The J_{sc} and V_{oc} are very important in tandem cell design. The J_{sc} follow the minimum value of the connected cells in series and V_{oc} follow the higher value of the connected cell. The J—V characteristics of the single CZTGS top-cell, the single CZTS bottom-cell and the whole CZTGS/CZTS tandem cell are shown together in Fig. 7. The photovoltaic parameters deduced from these characteristics are shown Table 4.

It is observed from Table 4 that the J_{sc} of the tandem cell is limited by the lower J_{sc} of the CZTGS top-cell because the top and bottom cells were current-mismatched. However, as the thickness of the top sub cell increases, the top cell current density, J_{sc} (top) increases and that of the bottom cell J_{sc} (bottom) decreases. This is because the thicker top cell absorbs more light at the expense of the bottom cell leaving less light to be transmitted to it. Consequently, current matching condition in this case can be achieved with increasing the CZTGS layer thickness while keeping that of the CZTS layer thickness constant. This results into the increase of J_{sc} (top) and a slight decrease in the J_{sc} (bottom). At an optimal CZTGS thickness of 0.65 μm the current matching condition is established with a current of 18.53 mA/cm^2 (Fig. 8). The photovoltaic parameters of the top, bottom and tandem solar cells of the current matching condition is presented in Table 5.

The open circuit voltage of the tandem cell is limited by the recombination in the space charge region of the junctions as shown in Fig. 9. It is important to note that the V_{oc} of the bottom sub-cell is almost independent of the variation of the thickness of top sub-cell. Using the approximate empirical expression by Green, ideally the fill factor is a function of the open circuit voltage [34]. Hence, the lower V_{oc} of the top sub-cell will result into a lower fill factor of the device. Since, the efficiency of the device is proportional to the fill factor, the combined efficiency of the tandem cell will reduce. In addition, because of the series connection of the cells, the efficiency of the tandem solar cell is limited by the solar cell that issues the lower current.

The quantum efficiency (QE) curves are shown in Fig. 10 for the top CZTGS single junction cell and CZTGS/CZTS tandem cell. In a similar report of Enam et al., (2017), QE signifies the portion of wavelength being converted into electron hole pair and collected as current [35]. Fig. 10 clearly shows that the CZTGS/CZTS tandem solar cell has better performance in terms of efficiency compared to CZTGS solar cell. The enhanced absorption of photon energy from the lower band gap of the bottom cell at longer wavelength and the higher band gap top cell at shorter wavelength of the tandem cell, results in photocurrent generation over a wide spectral range. Thus, improving the overall efficiency for the tandem structure.

3.4. Effect of temperature on the CZTGS/CZTS tandem solar cell

The performance of a solar cell is influenced by temperature since its performance parameters are influenced by it. The main temperature dependence in solar cells arises from variation of the open-circuit voltage with temperature. This voltage results from a balance between the overall recombination rate of carriers in the cell and the photogeneration rate [36]. As a result, the dominant recombination path can be studied via temperature-dependent current–voltage analysis. Assuming that the solar cell can be described with a one-diode model. Neglecting the parasitic resistances, the open-circuit voltage dependence on temperature is given by Eq. (7) [37].

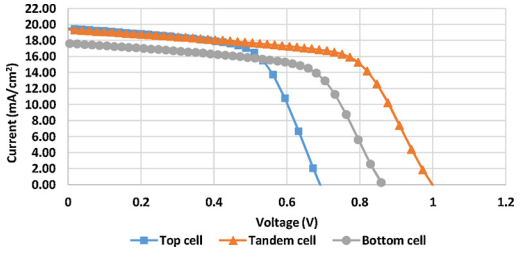

Fig. 7. J–V characteristics for the CZTGS top-cell, CZTS bottom-cell and CZTGS/CZTS tandem cell.

Table 4
Photovoltaic parameters of the top, bottom and tandem solar cells.

Solar cell parameters	Top cell (CZTGS)	Bottom cell (CZTS)	Tandem cell (CZTGS/CZTS)
V_{oc} (V)	0.86	0.68	1.04
J_{sc} (mA/cm^2)	17.39	19.72	19.37
FF (%)	63.31	62.72	63.54
η (%)	9.39	8.42	14.85

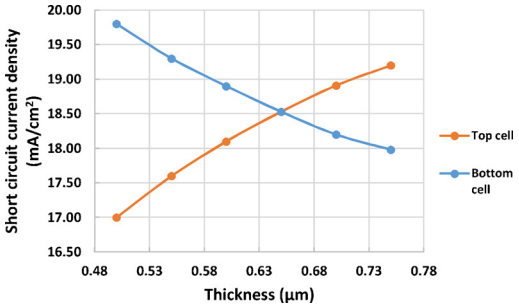

Fig. 8. Short circuit current densities of the top CZTGS and bottom CZTS solar cell as a function of the top CZTGS layer thickness.

Table 5
Photovoltaic parameters of the top, bottom and tandem solar cells under short-circuit current densities matching.

Solar cell parameters	Top cell (CZTGS)	Bottom cell (CZTS)	Tandem cell (CZTGS/CZTS)
V_{oc} (V)	0.68	0.67	1.35
J_{sc} (mA/cm^2)	18.53	18.53	18.53
FF (%)	60.15	62.70	62.17
η (%)	9.32	8.20	17.51

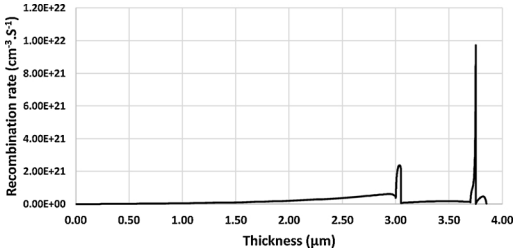

Fig. 9. Recombination rate of the CZTGS/CZTS tandem cell.

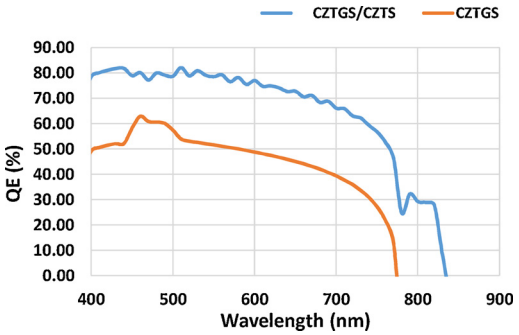

Fig. 10. External Quantum Efficiency of both CZTGS and CZTGS/CZTS tandem solar cell structure.

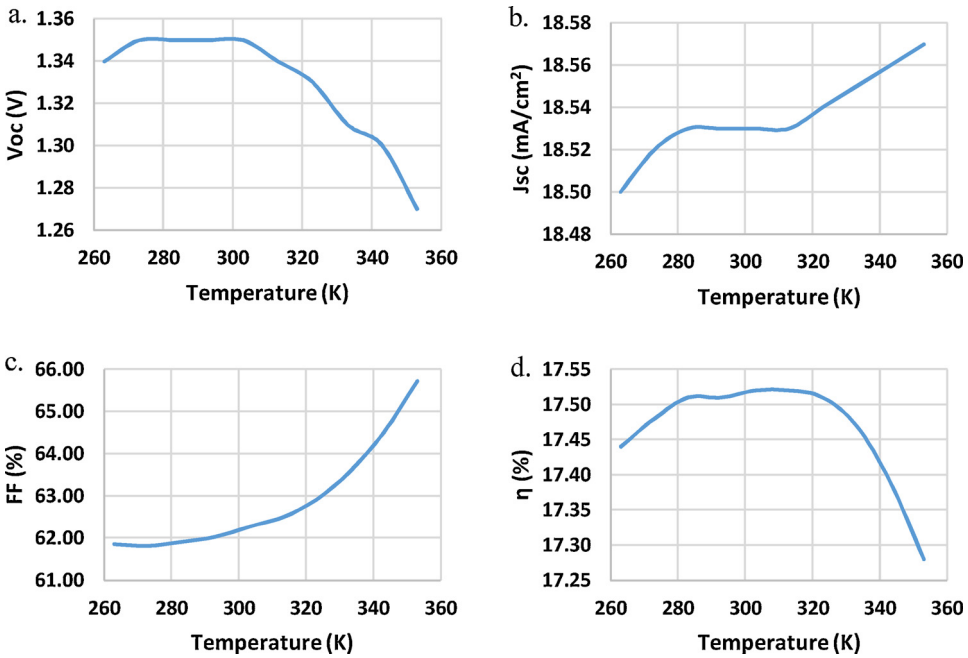

Fig. 11. a. Temperature effect on the tandem cell V_{oc}. b. Temperature effect on the tandem cell J_{sc}. c. Temperature effect on the tandem cell FF. d. Temperature effect on the tandem cell η.

$$V_o = \frac{nkT}{q} In\left(\frac{J_{sc}}{J_o} + 1\right) \tag{7}$$

Where J_{sc} is the short circuit current, J_o is the reverse saturation current, T is the temperature, q is the electronic charge and K is the Boltzmann constant and n is the ideality factor.

In terrestrial applications, solar cells are generally exposed to temperature varying from 283 K to 323 K [38]. However, in this work, we studied the effect of temperature variation on the tandem cell using a wider range between 263 K and 353 K. This is to accommodate more temperature extremes than the regular temperature range. The effect of temperature on photovoltaic parameters is presented in Fig. 11a–d.

Generally, it is observed that with increasing temperature, V_{oc} is decreasing (Fig. 11a) owing to the fact that the value of J_o increases exponentially with increasing $1/T$ causing V_{oc} to decrease with increasing T [39]. Apparently, the drop in V_{oc} with temperature, dominates the efficiency loss. In addition, Green, establishes the importance of the electron-hole product in recombination throughout the device, leading to a general formulation that temperature sensitivity is due to the open circuit voltage, accounting for 80–90% of the temperature sensitivity in the device [36]. However, increasing the temperature has a positive effect on the J_{sc}. The increase in temperature reduces the bandgap of the semiconductor which results into increase in the leakage current that enhances the short circuit current as shown in Fig. 11b. As the band gap decreases with temperature rise, more electron-hole pairs can potentially be photo-generated [34]. However, the effect of temperature increase on the short circuit current of the tandem cell is very small. The fill factor is observed to increase with increasing temperature (Fig. 11c). This could be attributed to the fact that the recombination junction offers an excellent series connection between the top and bottom sub-cells to eliminate shunting in each cell. The decrease in the efficiency of the tandem cell (Fig. 11d) with temperature is mainly controlled by the decrease of V_{oc}. At a temperature of 303 K, the performance of the CZTGS/CZTS tandem thin film solar cell appears to be optimal.

4. Conclusion

Numerical modeling and simulation of CZTGS/CZTS has been carried out in this research work using the Solar Cell Capacitance Simulator (SCAPS-1D). A systematic enhancement of the top cell CZTGS solar cell was carried out through the tuning of the band gap by using a non-toxic Ge and the variation of the electron affinity. An optimal band gap of 1.69 eV with its corresponding electron affinity of 4.19 eV of the CZTGS top cell was determined at a composition ratio of $Cu_2ZnSn_{0.8}Ge_{0.2}S_4$. Simulating the top cell with these parameters an efficiency of 9.39% was obtained. Also, the numerical simulation of CZTS bottom cell is carried out and an efficiency of 8.42% was obtained which is comparable to the previously reported experimental result. The top and bottom sub cells were coupled together to form a two-terminal monolithic tandem structure. An efficiency of 17.51% was achieved with the current matching conditions at a current density of 18.53 mA/cm^2 at a thickness of 0.65 µm. In addition, throughout the whole wavelength range, CZTGS/CZTS tandem cell's spectral response is higher than that of the single junction CZTGS cell. Finally, the temperature variation effect on the tandem cell was carried out. Generally, it was observed that at a temperature of 303 K, the efficiency of the

device was optimal. These results show that a monolithic tandem structure of CZTGS/CZTS can enhance the performance of a single junction CZTS solar cell by harnessing more of the spectrum of solar radiation that could have been wasted.

Acknowledgments

The authors acknowledge Prof. Marc Burgelman and his research group at the University of Gent for making SCAPS-1D available for our use.

Appendix A. Supplementary data

Supplementary material related to this article can be found, in the online version, at doi:https://doi.org/10.1016/j.ijleo.2018.09.033.

References

[1] V. Fthenakis, Sustainability metrics for extending thin-film photovoltaics to terawatt levels, MRS Bull. 37 (4) (2012) 425–430.
[2] M. Dhankhar, O.P. Singh, V.N. Singh, Physical principles of losses in thin film solar cells and efficiency enhancement methods, Renew. Sustain. Energy Rev. 40 (2014) 214–223.
[3] S.K. Wallace, D.B. Mitzi, A. Walsh, The steady rise of kesterite solar cells, ACS Energy Lett. 2 (4) (2017) 776–779.
[4] S.M. McLeod, C.J. Hages, N.J. Carter, R. Agrawal, Synthesis and characterization of 15% efficient CIGSSe solar cells from nanoparticle inks, Prog. Photovoltaics Res. Appl. 23 (11) (2015) 1550–1556.
[5] S. Das, K.C. Mandal, R.N. Bhattacharya, Earth-abundant $Cu_2ZnSn(S, Se)_4$ (CZTSSe) solar cells, Semiconductor Materials for Solar Photovoltaic Cells (Pp. 25–74), Springer International Publishing, 2016.
[6] M.A. Green, Y. Hishikawa, E.D. Dunlop, D.H. Levi, J. Hohl-Ebinger, A.W.Y. Ho-Baillie, Solar cell efficiency tables (version 51). Progress in photovoltaics, Res. Appl. 26 (2018) 3–12.
[7] M. Courel, O. Vigil-Galán, Different approaches for thin film solar cell simulation, Advanced Ceramic and Metallic Coating and Thin Film Materials for Energy and Environmental Applications (Pp. 245-286), Springer, Cham, 2018.
[8] W. Wang, M.T. Winkler, O. Gunawan, T. Gokmen, T.K. Todorov, Y. Zhu, D.B. Mitzi, Device characteristics of CZTSSe thin-film solar cells with 12.6% efficiency, Adv. Energy Mater. 4 (7) (2014) 1301465.
[9] A.D. Adewoyin, M.A. Olopade, M. Chendo, Enhancement of the conversion efficiency of Cu_2ZnSnS_4 thin film solar cell through the optimization of some device parameters, Optik-Int. J. For. Light Electron. Opt. 133 (2017) 122–131.
[10] Z. Zakaria, P. Chelvanathan, M.J. Rashid, M. Akhtaruzzaman, M.M. Alam, Z.A. Al-Othman, A. Alamoud, K. Sopian, N. Amin, Effects of sulfurization temperature on Cu_2ZnSnS_4 thin film deposited by single source thermal evaporation method, Jpn. J. Appl. Phys. 54 (8S1) (2015) 08KC18.
[11] F.M.T. Enam, K.S. Rahman, M.I. Kamaruzzaman, K. Sobayel, P. Chelvanathan, B. Bais, M. Akhtaruzzaman, A.R.M. Alamoud, N. Amin, Design prospects of cadmium telluride/silicon (CdTe/Si) tandem solar cells from numerical simulation, Optik-Int. J. For. Light Electron. Opt. 139 (2017) 397–406.
[12] M. Burgelman, K. Decock, A. Niemegeers, J. Verschraegen, S. Degrave, SCAPS Manual, (2016).
[13] M. Burgelman, P. Nollet, S. Degrave, Modeling polycrystalline semiconductor solar cells, Thin Solid Films 361–362 (2000) 527–532.
[14] S. Degrave, M. Burgelman, P. Nollet, Modelling of polycrystalline thin film solar cells: new features in SCAPS version 2.3, Proceedings of the 3rd World Conference on Photovoltaic Energy Conversion, WCPEC-3 (2003) 487–490.
[15] M. Burgelman, J. Verschraegen, S. Degrave, P. Nollet, Modeling thin-film PV devices, Prog. Photovoltaics Res. Appl. 12 (2–3) (2004) 143–153.
[16] S.R. Meher, L. Balakrishnan, Z.C. Alex, Analysis of Cu_2ZnSnS_4/CdS based photovoltaic cell: a numerical simulation approach, Superlattices Microstruct. 100 (2016) 703–722.
[17] N. Muhunthan, O.P. Singh, M.K. Thakur, P. Karthikeyan, D. Singh, M. Saravanan, V.N. Singh, Interfacial properties of CZTS thin film solar cell, J. Sol. Energy 476123 (2014) 1–8.
[18] M. Patel, A. Ray, Enhancement of output performance of Cu_2ZnSnS_4 thin film solar cells— a numerical simulation approach and comparison to experiments, Phys. B: Condens. Matter. 407 (21) (2012) 4391–4397.
[19] K. Wang, O. Gunawan, T. Todorov, B. Shin, S.J. Chey, Thermally evaporated Cu_2ZnSnS_4 solar cells, Appl. Phys. Lett. 97 (2012) 143508.
[20] M. Gloeckler, A.L. Fahrenbruch, J.R. Sites, Numerical modeling of CIGS and CdTe solar cells: setting the baseline, Proceedings of 3rd World Conference on Photovoltaic Energy Conversion, (2003), pp. 491–494 **a - c**.
[21] M. Djinkwi Wanda, S. Ouédraogo, F. Tchoffo, F. Zougmoré, J.M.B. Ndjaka, Numerical investigations and analysis of Cu_2ZnSnS_4 based solar cells by SCAPS-1D, Int. J. Photoenergy 2016 (2016).
[22] Y.H. Khattak, F. Baig, S. Ullah, B. Marí, S. Beg, H. Ullah, Enhancement of the conversion efficiency of thin film kesterite solar cell, J. Renew. Sustain. Energy 10 (3) (2018) 033501.
[23] B. Shin, O. Gunawan, Y. Zhu, N.A. Bojarczuk, S.J. Chey, S. Guha, Thin film solar cell with 8.4% power conversion efficiency using an earth-abundant Cu_2ZnSnS_4 absorber, Prog. Photovoltaics: Res. Appl. 21 (2013) 72–76.
[24] A. Mahfoud, S. Mekhilef, F. Djahli, Effect of temperature on the GaInP/GaAs tandem solar cell performances, Int. J. Renew. Energy Res. (IJRER) 5 (2) (2015) 629–634.
[25] Y.S. Lin, S.Y. Lien, C.C. Wang, C.H. Hsu, C.H. Yang, A. Nautiyal, D.S. Wuu, P.C. Tsai, S.J. Lee, Optimization of recombination layer in the tunnel junction of amorphous silicon thin-film tandem solar cells, Int. J. Photoenergy (2011) 2011.
[26] M. Elbar, S. Tobbeche, A. Merazga, Effect of top-cell CGS thickness on the performance of CGS/CIGS tandem solar cell, Sol. Energy 122 (2015) 104–112.
[27] K. Kim, J. Gwak, S.K. Ahn, Y.J. Eo, J.H. Park, J.S. Cho, M.G. Kang, H.E. Song, J.H. Yun, Simulations of chalcopyrite/c-Si tandem cells using SCAPS-1D, Sol. Energy 145 (2017) 52–58.
[28] O.K. Simya, A. Mahaboobbatcha, K. Balachander, A comparative study on the performance of Kesterite based thin film solar cells using SCAPS simulation program, Superlattices Microstruct. 82 (2015) 248–261.
[29] M. Singh, T.R. Rana, J. Kim, Fabrication of band gap tuned $Cu_2Zn(Sn_{1-x}Ge_x)(S,Se)_4$ absorber thin film using nanocrystal-based ink in non-toxic solvent, J. Alloys Compd. 675 (2016) 370–376.
[30] D.B. Khadka, J. Kim, Band gap engineering of alloyed $Cu_2ZnGe_xSn_{1-x}Q4$ (Q=S, Se) films for solar cell, J. Phys. Chem. C 119 (4) (2015) 1706–1713.
[31] A.D. Adewoyin, M.A. Olopade, M. Chendo, Prediction and optimization of the performance characteristics of CZTS thin film solar cell using band gap grading, Opt. Quantum Electron. 49 (10) (2017) 336.
[32] S.R. Kodigala, Thin Film Solar Cells from Earth Abundant Materials: Growth and Characterization of $Cu_2ZnSn(SSe)_4$ Thin Films and Their Solar Cells, Elsevier, New York, 2014.
[33] P. Singh, N.M. Ravindra, Temperature dependence of solar cell performance—an analysis, Sol. Energy Mater. Sol. Cells 101 (2012) 36–45.
[34] M.A. Green, Solar Cells: Operating Principles, Technology, and System Applications, Prentice-Hall, Inc., New Jersey, 1982.
[35] F.M.T. Enam, K.S. Rahman, M.I. Kamaruzzaman, K. Sobayel, P. Chelvanathan, B. Bais, M. Akhtaruzzaman, A.R.M. Alamoud, N. Amin, Design prospects of cadmium telluride/silicon (CdTe/Si) tandem solar cells from numerical simulation, Optik-Int. J. For. Light Electron. Opt. 139 (2017) 397–406.

[36] M.A. Green, General temperature dependence of solar cell performance and implications for device modelling, Prog. Photovoltaics Res. Appl. 11 (5) (2003) 333–340.
[37] A.D. Adewoyin, M.A. Olopade, M.A.C. Chendo, A comparative study of the effect of transparent conducting oxides on the performance of Cu_2ZnSnS_4 thin film solar cell, J. Comput. Electron. 17 (1) (2018) 361–372.
[38] P. Singh, S.N. Singh, M. Lal, M. Husain, Temperature dependence of I–V characteristics and performance parameters of silicon solar cell, Sol. Energy Mater. Sol. Cells 92 (12) (2008) 1611–1616.
[39] R.H. Bube, A.L. Fahrenbruch, Fundamentals of Solar Cells, Academic Press, London, New York, 1983.